Research Square

Preprints are preliminary reports that have not undergone peer review.
They should not be considered conclusive, used to inform clinical practice,
or referenced by the media as validated information.

Novel Lytic Enterococcus Phage as a Biocontrol Strategy for Multidrug-Resistant Enterococcus faecalis Biofilms on Food-Contact Surfaces: Genomic and Functional Insights

Dina El-Sayed
Cairo University
Rasha Samir Mohamed
Cairo University
Marwa N. Ahmed
marwanabil@nu.edu.eg

Nile University
Mokhtar Gomaa
National Research Centre
Mohamed El-Telbany
National Institute of Infectious Diseases, Japan Institute for Health Security
Yoshimitsu Masuda
Kyushu University
Ken-ichi Honjoh
Kyushu University
Eman M. Taher
Cairo University

Article

Keywords: Enterococcus faecalis, bacteriophage BV26, biofilm inhibition, biofilm eradication, dairy industry, biocontrol, food safety, lytic phage

Posted Date: October 5th, 2026

DOI: https://doi.org/10.21203/rs.3.rs-10789862/v1

License: This work is licensed under a Creative Commons Attribution 4.0 International License.
Read Full License

Additional Declarations: No competing interests reported.

Novel Lytic Enterococcus Phage as a Biocontrol Strategy for Multidrug-Resistant *Enterococcus faecalis* Biofilms on Food-Contact Surfaces: Genomic and Functional Insights

Dina El-Sayed[a], Rasha Samir Mohamed[a], Marwa N. Ahmed[b,a*], Mokhtar Gomaa[c], Mohamed El-Telbany [d], Yoshimitsu Masuda[e], Ken-ichi Honjoh[e], Eman M. Taher[f]

[a]Department of Agricultural Microbiology, Faculty of Agriculture, Cairo University, Giza, 12613, Egypt.

[b]Biotechnology Research and Innovation Centre (BRIC), School of Biotechnology, Nile University, Giza, 12588, Egypt.

[c]Centre of Scientific Excellence for Influenza Viruses, National Research Centre, Giza, Egypt

[d]Department of Drug Development, National Institute of Infectious Diseases, Japan Institute for Health Security, Tokyo, Japan.

[e]Department of Bioscience and Biotechnology, Faculty of Agriculture, Kyushu University, Fukuoka 819-0395, Japan.

[f]Department of Food Hygiene and Control, Faculty of Veterinary Medicine, Cairo University, Giza, 12211, Egypt

*Corresponding author:

Marwa N. Ahmed, PhD

Associate Professor

School of Biotechnology

Nile University

12588

Giza, Egypt

marwanabil@nu.edu.eg

https://orcid.org/0009-0009-3685-6859

Abstract

Enterococcus faecalis is one of the most prevalent biofilm-forming bacteria that persists on dairy processing surfaces, posing significant food safety and health concern. In this study, two lytic bacteriophages, BV26 and BV34, were isolated and characterized from sewage for use as biocontrol for *E. faecalis*. Both types of phages belong to the family of *Siphoviridae*, as observed by transmission electron microscopy. The level of stability for the phage BV26 was evaluated to determine its potential biocontrol effectiveness at a wide range of pH levels (3 to 12), UV resistance, and thermal stability up to 50 °C. Whole-genome sequencing of BV26 revealed their predicted coding sequences, with no detectable virulence or antimicrobial resistance genes, supporting its safety for biocontrol applications. Comparative genomic and phylogenetic analyses indicated that BV26 represents a distinct lineage among *Enterococcus* phages. BV26 was tested for anti-biofilm activity against planktonic and biofilm-bound *E. faecalis*. In microtiter-plate biofilm formation assays, the anti-biofilm effect of phage BV26 was most pronounced when BV26 was added at a multiplicity of infection of 100. In a dairy processing surface biofilm formation assay, BV26 decreased *E. faecalis* biofilm formation by more than 3 $\log_{10}$ CFU/coupon after five days. These findings highlight the novelty and potential of phage BV26 as a safe, stable, and effective biocontrol agent for preventing and eliminating *E. faecalis* biofilms in dairy processing facilities.

Keywords

Enterococcus faecalis; bacteriophage BV26; biofilm inhibition; biofilm eradication; dairy industry; biocontrol; food safety; lytic phage

1. Introduction

Antimicrobial resistance (AMR) is a major global public health concern, driven by the continued emergence and spread of bacteria that are resistant to multiple clinically important antibiotics. In addition, resistant bacteria and antimicrobial resistance genes can transfer between humans, animals, food-producing systems, and the environment, allowing them to persist and circulate across different settings [1]. Environmental habitats such as water, soil, animal waste, and food-processing environments can therefore serve as important reservoirs for resistant bacteria and provide opportunities for their further dissemination and exchange of resistance determinants[2]. Moreover, biofilm formation by pathogenic bacteria exacerbates the AMR resilience, as cells growing within the extracellular polymeric matrix are generally more tolerant to antimicrobial treatments than their planktonic counterparts, allowing them to persist under conditions that may effectively eliminate free-living cells [3-5].

Among the bacterial groups of particular concern in food and environmental settings are *Enterococci*. *Enterococci* are ubiquitous, commensal bacteria that naturally colonize the gastrointestinal tracts of humans and animals. Beyond their role as members of the gut microbiota, they are highly adaptable organisms that persist in a wide range of environmental niches, including soil, water, plants, and food-processing environments, reflecting their remarkable resilience and ecological adaptability [6]. In dairy environments, *Enterococcus species,* most notably *E. faecalis,* are commonly isolated due to their pronounced ability to withstand adverse conditions, including high temperatures, elevated salt concentrations, and wide pH ranges. Such intrinsic stress tolerance, combined with their metabolic versatility, facilitates their survival during dairy processing and storage. Furthermore, lapses in sanitation protocols can promote their persistence in dairy processing facilities, where they readily adhere to abiotic surfaces and develop structured biofilms [7, 8].

The formation of *E. faecalis* biofilms represents a substantial challenge across multiple industries, particularly within the dairy sector, as they enhances the microbial resistance to cleaning and disinfection procedures, contributing to their continued occurrence on downstream processes, causing blockages, insufficient heat transfer, and erosion of milking and processing equipment, in addition to affecting product shelf life, quality and overall safety [9].

Experimental and industrial observations further substantiate their biofilm-forming potential, for instance**, [10]** demonstrated that several *Enterococcus spp*. were able to develop multispecies dairy biofilms on stainless steel surfaces within a bioreactor supplied with microfiltered milk. Likewise,[11] reported that *E. faecalis* was capable of forming biofilms on stainless-steel surfaces in a commercial

cheese manufacturing facility within 1 to 8 days of contact at temperatures ranging from 10 °C to 43 °C. Furthermore, *E. faecalis* possesses both intrinsic and acquired virulence determinants, along with notable resistance to multiple antibiotics, including aminoglycosides and cephalosporins, as well as the increasing occurrence of vancomycin-resistant enterococci (VRE) [12]. Additionally, it may pose a food safety risk by producing and accumulating biogenic amines (BAs), such as tyramine and putrescine, which can be cytotoxic and genotoxic to intestinal cells, potentially contributing to foodborne intoxication [13].

One commonly employed strategy to mitigate biofilm formation involves the implementation of effective sanitation protocols combining detergents and chemical sanitizers. However, repeated or sub-lethal exposure to these sanitizing agents may trigger adaptive responses in microorganisms, potentially resulting in increased tolerance, cross-resistance to antibiotics, and enhanced persistence of biofilm-associated cells [14].

In this context, bacteriophages (phages) have emerged as promising and sustainable biocontrol alternatives. Bacteriophages are classified as lytic or lysogenic according to their life cycles. Unlike lysogenic phages, lytic phages exclusively follow the lytic cycle, leading solely to the destruction of their host bacteria [15]. Due to their high host specificity, phages selectively target pathogenic bacteria without disrupting beneficial microflora and starter culture, while preserving the sensory attributes and quality characteristics of the food products [16]. Nonetheless, within biofilms formed on processing equipment and abiotic surfaces, phages initially infect surface-associated bacteria and replicate intra-cellularly. The resulting progeny penetrates deeper biofilm layers, facilitating sequential bacterial lysis. In addition, phage-encoded depolymerases can degrade the extracellular polymeric substance (EPS) matrix, further enhancing access to embedded cells. This cascading infection dynamic provides an effective strategy for reducing *E. fecalis* biofilm formation in dairy processing systems [17].

Hence, this study aimed to isolate and comprehensively characterize two bacteriophages targeting *E. faecalis*. The most stable phage was selected for whole-genome sequencing to elucidate its genetic composition and assess its safety and suitability for biocontrol applications. Subsequently, phage BV26 was evaluated for its anti-biofilm efficacy against *E.* faecalis in both planktonic cultures and biofilms formed on stainless steel surfaces. Hitherto, this study represents one of the few comprehensive investigations evaluating bacteriophage application in both biofilm inhibition and eradication models of *E.* faecalis on stainless steel surfaces simulating dairy processing environments, thereby highlighting its practical relevance for controlling *E. faecalis* biofilms in the dairy sector.

2. Materials and Methods

2.1. Bacterial strains

Enterococcus faecalis strain was previously isolated from milk at the Food Hygiene and Control Department, Faculty of Veterinary Medicine, Cairo University, Giza and molecularly identified.

2.2. Bacteriophages isolation and purification

For isolation of *E. faecalis* bacteriophages, ten sewage samples were collected from Giza governorate, filtered using a 0.45 µm filter (Millipore, Merck, and Darmstadt, Germany). 10 mL of each filtered sewage sample was mixed with 5 mL of an overnight culture of *E. faecalis* and applied to 50 mL of tryptone soya broth (TSB), incubated at 37 ºC with shaking. After 24 h of incubation, bacterial cultures were spun down for 15 min at 6000 xg, the supernatants were separated, filtered using a syringe filter 0.45 µm, and tested for phage lytic activity by spot test [18]. Briefly, 5 µL of phage filtrate was spotted onto a layer inoculated with *E. faecalis*. A clear zone of plaques on the bacterial lawn indicates the presence of bacterial-specific lytic phage.

The plaque assay method was used for the *E. faecalis* purification lysates [19]. 10-fold serial dilutions of the filtered phage suspension were prepared in phosphate-buffered saline (PBS; 8 g/L NaCl, 0.2 g/L KCl, 1.44 g/L Na_2HPO_4, and 0.24 g/L KH_2PO_4, pH 7.4). 0.5 mL of each dilution was mixed with 0.5 mL of an overnight culture of *E. faecalis* and 5 mL of semi-solid tryptone soya agar (TSA) (0.7% w/v) and overlaid on top of a solidified TSA base layer (2% w/v) plates and incubated at 37 °C. After 24 h, a single plaque was picked and suspended in 50 mL of an overnight culture of *E. faecalis*, and incubated with shaking. after 24 h incubation at 37 ºC, the culture was spun down at 10000 ×g for 30 min, and the supernatant was filtered through a 0.2 µm syringe filter. The purification procedure was repeated thrice to ensure the phage lysate purity.

2.3. Transmission Electron Microscopy (TEM)

The sucrose cushion concentrated phage was applied on the surface of a lacey carbon-supported copper grid (Sigma-Aldrich, Germany), negatively stained with 2% (w/v) phosphotungstate at pH 7.2, and air dried. The stained grid was micro-analysed using the JEM-2100 HRT high-resolution TEM electron microscope (Jeol Ltd, Japan) at the Electron Microscopy Unit, National Research Center, Giza, Egypt.

2.4. Direct spot test for host-range determination

For host range testing, volume of 200 µl containing $1.5x10^8$ colony forming units (CFU) of each bacterial strain was suspended in 5 mL of molten 0.7% TS soft agar (~45 °C), and seeded over a solidified 2% TSA base 90 mm plate. After 30 min solidification at 25 °C, a volume of 10 µl of phage

lysate containing ~10^6 plaque forming units (PFU) was spotted on the bacterial lawn, then incubated in 37 °C. After 24 h, phage activity was recorded as clear zones, the assay was done as triplicate for each bacterial strain.

2.5. Environmental stability of isolated bacteriophages

The stability of *E. faecalis* phages was evaluated under different environmental stress conditions, including ultraviolet radiation (UV), pH, and temperature [20]. a Bio-Link BLX-E254 UV crosslinker (Vilber Lourmat, France) was used for UV treatment assay, two triplicate sets of 5 ml each (~10^8 PFU/Ml) were exposed to 254-nm UV at an energy dose of 15 Joules for 30 and 60 min, untreated phage was used as control. For PH stability assay, a volume of 1mll containing ~ 10^8 PFU/mL were suspended in 10 ml of TSB adjusted at different PH (2-12), a triplicate phage set with neutral PH was used as control. Thermal stability were tested with incubation of triplicate phage sets at 25,40, 50, 60, 70, and 80 °C for one hour. Phages were quantified with plaque double layer agar assay after incubation at 37 °C for 24 h.

2.6. Phage concentration and nucleic acid extraction

The sucrose cushion method was used to concentrate the E. faecalis bacteriophages. A volume of 50 mL of each phage was applied on top of 6 mL of 20% sucrose in three different tubes and subjected to ultracentrifugation process using the Sorvall MTX 150 mini-ultracentrifuge (Thermo Fisher Scientific) (100,000× g at 4 °C for 2 h). Finally, phage pellets were totally resuspended in 0.5 mL PBS (100X concentrated). A volume of 200 µl of concentrated phage was subjected to nucleic acid extraction using the MagMAX™ Total Nucleic Acid Isolation Kit (Applied Biosystems, California, USA), following the manufacturer's instructions, with the aid of KingFisher™ Flex Purification System (Thermo Fisher Scientific, Rockford, IL, USA). Phage genomic nucleic acid was eluted in 50 µL nuclease-free water, and the DNA concentration was assessed using the Qubit dsDNA BR (Broad Range) Assay Kit with the aid of Qubit™ 3 Fluorometer (Thermo Fisher Scientific, Waltham, MA, USA).[20]

2.7. Genome Sequencing and Assembly

The extracted DNA was subsequently prepared for sequencing using the Illumina TruSeq DNA Nano Library Preparation Kit (Illumina, San Diego, CA, USA) and sequenced on an Illumina MiSeq platform, generating approximately 50× sequencing coverage. The assembled contigs were generated from raw sequencing following standard quality control and trimming steps using Fastp **[21]**. Assembly was performed using CLC Genomics Workbench version 25.0.2 (QIAGEN, Aarhus, Denmark). To identify viral sequences, assembled contigs were analyzed using CheckV [22]. These

tools enabled robust viral classification based on genome features and hallmark gene content. Two independent methods were used to assess viral genome completeness. The first method is an AAI-based completeness assessment in which amino acid identity (AAI) values were determined by aligning translated contigs to a curated viral genome database using PHASTER (PHAge Search Tool Enhanced Release) [23] . For each contig, the top hit identity score (ID), expected genome length, completeness percentage, confidence level, and the number of matching protein-coding genes were documented.

The second approach involved HMM-based completeness, where hidden Markov model (HMM) profiles from the CheckV marker gene database were used to identify conserved viral protein domains. The number of HMM hits and predicted completeness range (lower and upper bounds) were recorded.

2.8. Genome Annotation

The assembled phage genome was functionally annotated using two complementary approaches to ensure annotation accuracy and completeness. PHASTEST (PHAge Search Tool with Enhanced Sequence Translation) [24] was employed for bacteriophage genome annotation, including the prediction of coding sequences (CDSs), tRNAs, and rRNAs, and the assignment of putative functions based on curated protein databases. In parallel, PhageScope was also used as a complementary phage-specific database and annotation resource to further assess and characterize the predicted phage proteins and genomic features. Functional annotation was further supported by BLASTp searches against the NCBI non-redundant (nr) protein database. Antimicrobial resistance genes and virulence factors were screened using the Comprehensive Antibiotic Resistance Database (CARD) [25] and the Virulence Factor Database (VFDB) [26], respectively. The annotated genome map of phage BV26 was subsequently constructed using PhageScope [27].

2.9. Comparative Genomics

The complete genome sequence of phage BV26 was compared to publicly available phage genomes using the BLASTn algorithm at NCBI to identify the most closely related reference genomes. Average Nucleotide Identity (ANI) values between the sequenced phage and its closest relatives were calculated using both the JSpeciesWS online service (Richter et al. 2016) and the FastANI tool in Proksee [28]. The whole-genome sequence of the tested phage was deposited into the NCBI GenBank database and identified as *Enterococcus* phage BV26 under the accession number “PZ136974”.

2.10. Comparative Proteomic and Phylogenetic Analysis

For the global proteomic comparison, the complete proteome of BV26 was analyzed using ViPTree (Virus Proteomic Tree Server)[29] which computes genome-wide similarity based on normalized

tBLASTx scores between all proteins encoded in the phage genomes. The resulting tree was visualized to determine the placement of BV26 among members of the class *Caudoviricetes*. In addition, tBLASTx analysis was performed to identify homologous regions across all six reading frames of the translated nucleotides in of BV26 and closely related phages.

To investigate the evolutionary relatedness of the isolated phage BV26 with other related phages, phylogenetic and proteomic analyses were performed based on the amino acid sequences of the large terminase subunit (TerL). The protein sequences were retrieved from the NCBI GenBank database and aligned using ClustalW [30]. Phylogenetic trees were constructed using the Neighbor-Joining method with 1000 Bootstrap replicates to evaluate branch support values. Bootstrap values exceeding 75% were represented as bubbles in the resulting tree. The tree was visualized using iTOL v7 (interactive tree of life)[31].

2.11. Anti-Biofilm Activity Assay

Biofilm formation and quantification were assessed using a microtiter plate-based crystal violet assay [32], with some modifications; *E. faecalis* was grown overnight aerobically in LB broth at 37°C. The culture was adjusted to the exponential growth phase ($OD_{600} \approx 0.6$ to 0.8) and then diluted to reach a final concentration of about 10^6 CFU/ml and distributed as 100 µl/ well in a sterile 96-well flat-bottom microtiter plate. Different multiplicities of infection (MOIs) 0.01, 0.1, 1,10, and 100 of bacteriophages were prepared in sterile phosphate buffered solution (PBS), then applied as 6 replicates on the bacterial wells, 6 wells were left as control for bacterial growth without phage treatment. The plates were incubated statically at 37°C for 24 and 48 h to allow biofilm formation. Following incubation, planktonic cells were carefully removed by aspiration. Wells were gently washed three times with 200 µL sterile PBS to remove non-adherent cells.

Biofilms were stained with 150 µL/well of 0.1% (w/v) crystal violet solution at room temperature for 15 min. Excessive stain was removed, and wells were washed three times with PBS to eliminate unbound dye. The bound crystal violet was solubilized by adding 200 µL/well of 30% (v/v) acetic acid with gentle shaking at room temperature for 15–20 min. Biofilm mass was quantified by measuring the optical density at 570 nm (OD_{570}) using a microplate reader. The absorbance values were considered proportional to the total biofilm mass. Biofilm reduction was calculated relative to untreated bacterial control wells.

3. Results

3.1. Phenotypic characteristics and host range of BV26 and BV34

Two different lytic phages of *Enterococcus faecalis* were isolated from sewage samples and morphologically characterized using TEM examination. Phages appeared to have different sizes (Fig. 1). Both BV26 and BV34 possess hexagonal heads (40.73*48.67 nm) and (70.56*60.53 nm) respectively, and long non-contractile tails (~205 nm). The BV26 and BV34 morphology strongly suggests that both phages belong to the *Siphoviridae* family.

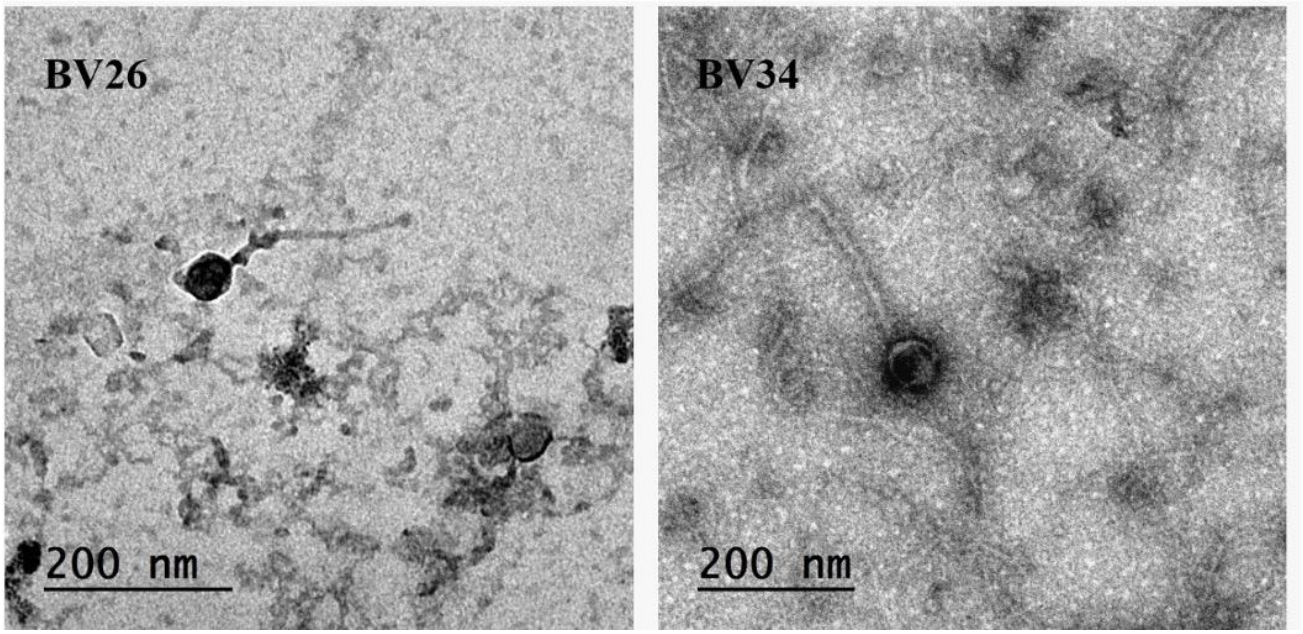

Fig 1. Transmission electron microscopy (TEM) images of the lytic bacteriophages BV26 and BV34 infecting *Enterococcus faecalis.* Both phages exhibit an icosahedral (hexagonal in projection) capsid and a long, flexible, non-contractile tail, characteristic of siphovirus-like morphology. Scale bars = 200 nm.

Host range analysis demonstrated the narrow host specificity of BV26 and BV34. Two *E. faecalis* strain, eight E. *faecium* strains, one *E. lactis*, one *E. massiliensis* and one *E. hulanensis* strain were examined using a direct spot test assay. Both phages infected their original *E. faecalis* host strain, while none of the other tested isolates showed susceptibility or supported phage propagation (Table 1).

Table 1; Host range for the BV26 and BV34 *E. faecalis* bacteriophages.

Serial	Bacterial strains	Accession number	Enterococcus phage BV26	Enterococcus phage BV34
1	*E. faecalis* **(host)**	-	+	+
2	*E. faecalis*	ATCC 19433	-	-

3	*E. faecium*	PX 952697	-	-
4	*E. faecium*	PX 952698	-	-
5	*E. faecium*	PX 952699	-	-
6	*E. faecium*	PX 952700	-	-
7	*E. faecium*	PX 952701	-	-
8	*E. faecium*	PX 952702	-	-
9	*E. faecium*	PX 952703	-	-
10	*E. faecium*	OQ709412	-	-
11	*E. lactis*	OQ709413	-	-
12	*E. massiliensis*	OQ709414	-	-
13	*E. hulanensis*	PQ497572	-	-

3.2. EV26 and EV34 tolerance to different environmental conditions

Temperature, UV radiation, and pH are important influences that affect the durability and virulence of bacteriophages towards their bacterial host. In this study, BV26 and BV34 showed adaptive environmental features. Both phages exhibited significant endurance across a wide pH range (4–12). Notably, BV26 retained activity even under low acidic conditions (up to pH 3), whereas BV34 showed higher delicacy to acidic conditions. (Fig. 2A).This tolerance to a wide pH range suggests a realistic phage therapy application within the gastrointestinal tract. Both phages BV26 and BV34 are approaching the same thermal tolerance model (Fig. 2B). They remained stable up to 50 °C, but their activity decreased remarkably at 70 °C, and total loss of activity occurred at 80 °C for BV34, which supports its potential for applications in environments with different temperatures. Phages' tolerance to UV radiation was also examined (Fig. 2C). The two phages showed no detectable reduction after 60 min of UV exposure. This UV tolerance ability should be considered when applying phage on the surfaces where UV sterilization will not inactivate the phage.

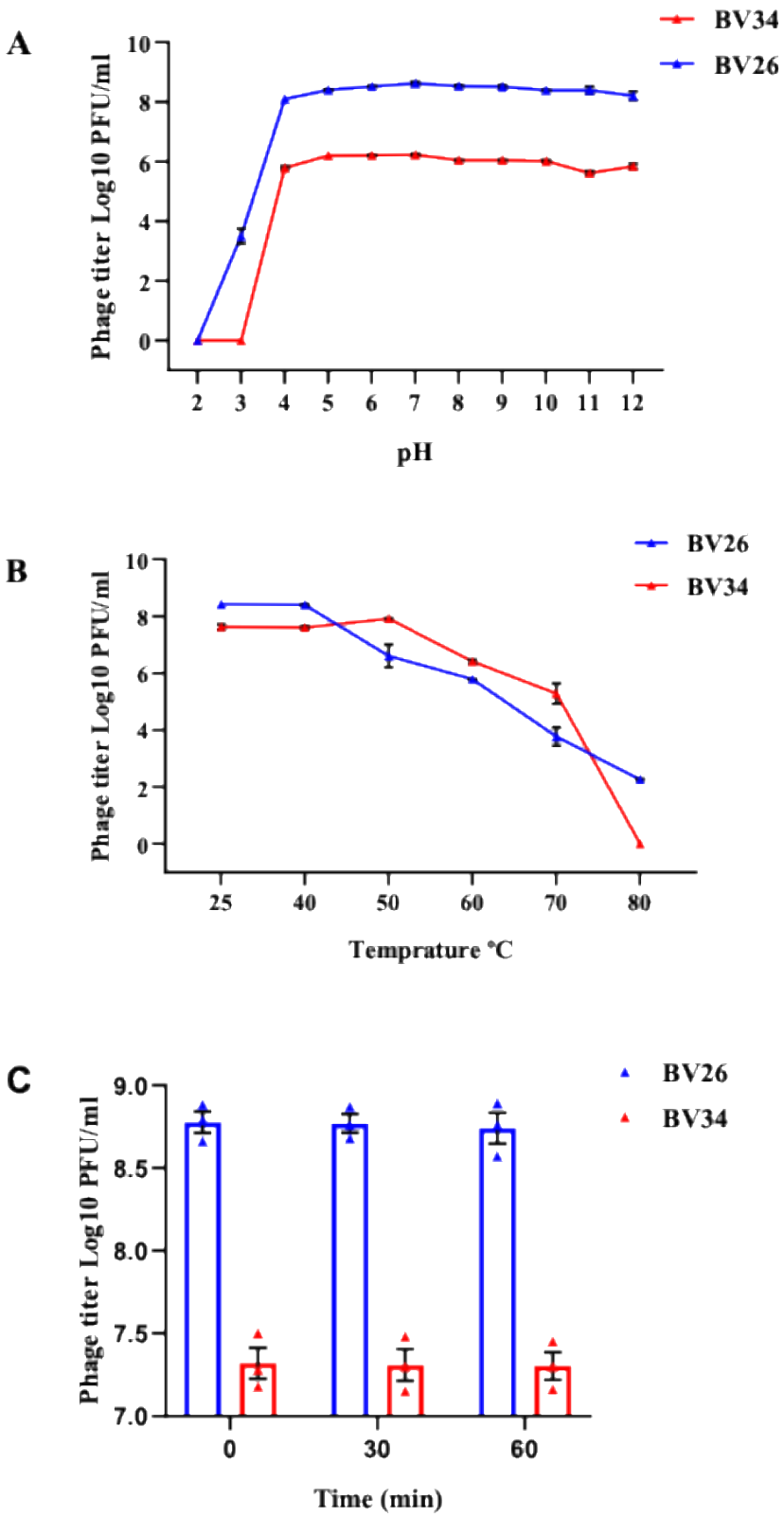

281

282 Fig. 2. Environmental stability of *Enterococcus faecalis* bacteriophages BV26 and BV34. Phage
283 stability was assessed following exposure to different pH values (2–12) (A), temperatures (25–80 °C)

(B), and UV irradiation (254 nm) for 30 and 60 min (C)**.** Surviving phages were quantified by the double-layer agar assay and expressed as PFU/mL (mean ± SD).

3.3. Genome Assembly and Completeness Assessment

Sequencing and assembly of the *Enterococcus* phage BV26 genome yielded a single contig of 41,165 bp**,** with a GC content of 34.91%**.** Completeness assessment using both AAI-based and HMM-based approaches indicated that the assembled sequence represents a complete phage genome, with no evidence of genomic contamination or truncation. The complete phage genome extended from nucleotide 1 to 41,165 and contained 66 predicted coding sequences (CDSs)**,** all of which showed significant similarity to phage-associated proteins in the NCBI non-redundant database. No tRNA genes were identified within the genome, and no bacterial proteins or host-derived sequences were detected, further supporting the absence of detectable bacterial DNA contamination. No att site sequences were identified, consistent with the absence of an identifiable integration site in the assembled genome.

Comparative sequence analysis revealed high similarity between BV26 and several *Enterococcus* phages, with the highest proportion of homologous sequences corresponding to *Enterococcus* phage vB_EfaS_Paulomi **(**93%) Overall, homologous sequences were identified among 25 distinct phage species, predominantly infecting *Enterococcus*, indicating that BV26 shares genetic features with a diverse group of enterococcal phages. The finding that 100% of the predicted CDSs had phage-associated homologues further supports the viral origin of the assembled genome and provides evidence for its close evolutionary relationship with previously characterized enterococcal phages.

3.4. Genome Annotation

Functional annotation categorized the predicted proteins into several functional modules based on their predicted roles (Fig. 3A & B). The largest functional category comprised genes involved in structural assembly, with 9 CDSs dedicated to virion morphogenesis, including capsid protein, tail length tape-measure protein, minor tail proteins, tail fiber protein, tail tip protein, and tail assembly protein. The presence of a capsid maturation protease further supports proper virion assembly.

DNA replication and lysis functions each accounted for 6 CDSs. The replication module included genes encoding DNA helicase, DNA polymerase, exonuclease, and single-stranded DNA binding protein, suggesting a well-equipped DNA replication machinery. The lysis module contained genes potentially involved in host lysis, including holin and lysin homologs.

315 The packaging module comprised 3 CDSs, including terminase subunits essential for DNA
316 encapsidation. Regulatory functions were represented by 3 CDSs, including a putative transcriptional
317 regulator. Integration-related functions and immune system components were each represented by a
318 single CDS.

319 A substantial portion of the genome (37 CDSs) consisted of genes encoding hypothetical proteins with
320 no assigned function, reflecting the diverse and partially uncharacterized nature of phage genetic
321 repertoires. Notably, no infection-related genes were identified in the genome, consistent with the
322 strictly lytic lifestyle of the phage. The functional distribution highlights the modular organization
323 typical of *Caudoviricetes* phages and provides insights into the replication strategy and structural
324 complexity of phage BV26. Table S1 supplementary file shows complete list of predicted coding
325 sequences in *Enterococcus* phage BV26 genome with predicted functions.

A

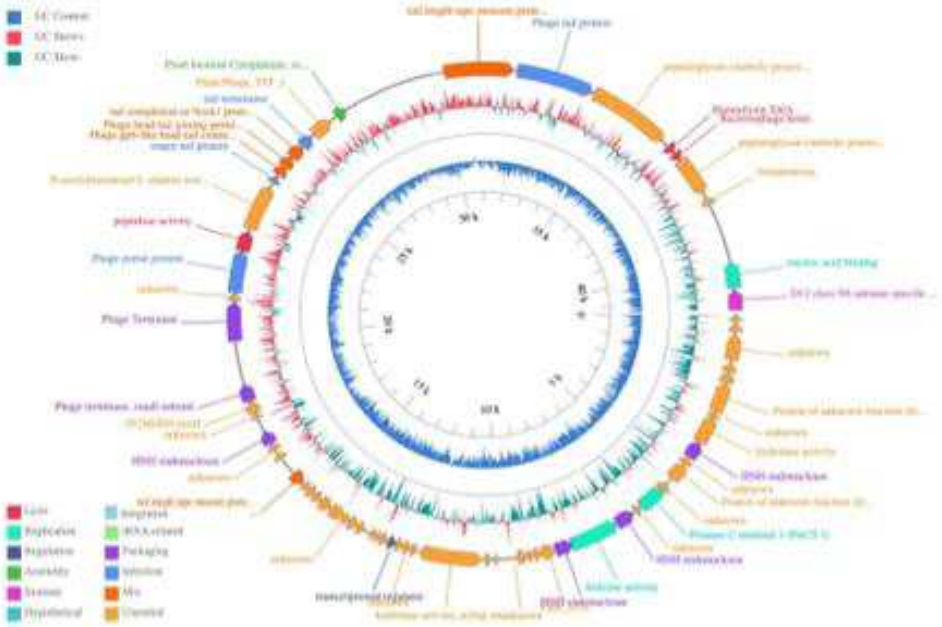

B

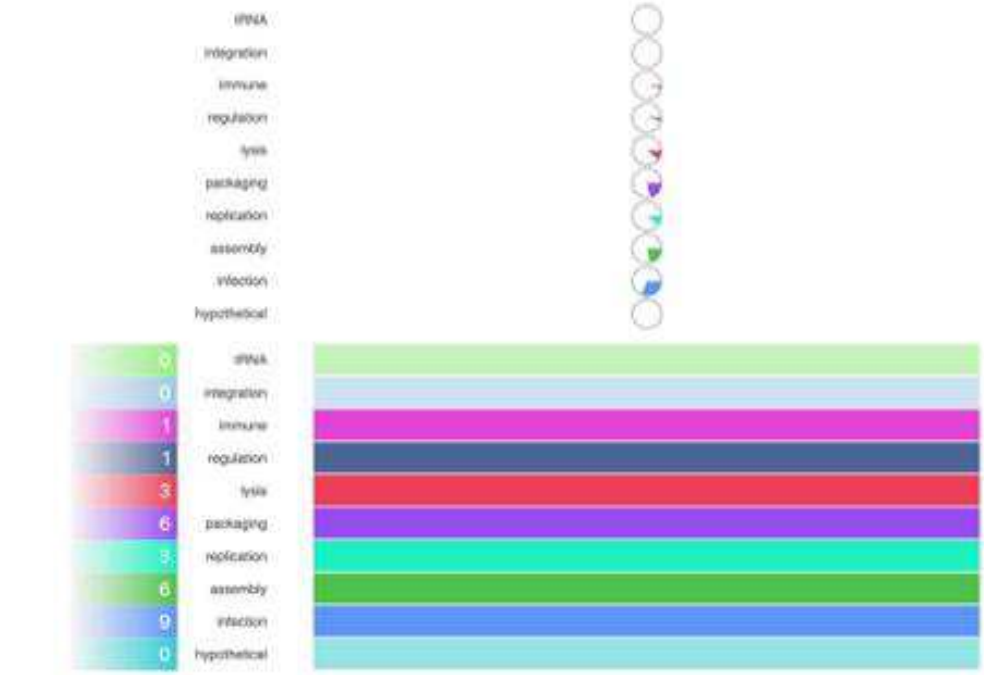
tRNA
integration
immune
regulation
lysis
packaging
replication
assembly
infection
hypothetical
0 tRNA
0 integration
1 immune
1 regulation
3 lysis
6 packaging
3 replication
6 assembly
9 infection
0 hypothetical

326

Fig.3. Genome map and functional annotation of bacteriophage BV26. Circular genome representation of bacteriophage BV26 showing predicted open reading frames (ORFs) and their functional classification. Genes are color-coded according to their predicted functions, including structural proteins (head, tail, portal, fiber), lysis-related proteins (holin and endonuclease), DNA packaging proteins (terminase), and phage-like proteins, while numerous ORFs encode hypothetical proteins with unknown functions. The inner rings represent GC content (black) and GC skew (green and purple), indicating nucleotide composition variation across the genome (A), and functional classification of predicted coding sequences (CDSs) in the *Enterococcus faecalis* phage BV26 genome. Genes were categorized based on their predicted biological functions, including DNA packaging, replication, regulation, lysis, structural assembly, and hypothetical proteins. The number of genes assigned to each functional category is indicated (B).

3.5.Comparative Genomics

Comparative genomic analysis based on ANI% revealed that phage BV26 shares relatively low nucleotide similarity with previously reported *Enterococcus* phages (Fig. 4A). The ANI heatmap demonstrates distinct clustering patterns, where closely related phages group together into well-defined clusters. Notably, BV26 exhibited a maximum ANI value of 91% with its closest relative, phage vB_EfaS_Paulomi. Despite this level of similarity, BV26 forms a separate branch within the dendrogram, indicating a clear genomic divergence from other analyzed phages.

Genome synteny analysis was conducted to evaluate structural conservation between BV26 and one of its closest relatives, vB_EfaS_Paulomi. The synteny analysis revealed several homologous genomic regions shared between the two phages, indicating partial conservation of gene organization (Fig. 4B). These conserved blocks likely correspond to essential functional modules such as DNA packaging, structural protein assembly, and replication. Despite these shared regions, substantial genomic rearrangements and divergent segments were observed across the genomes. Several genomic regions in BV26 lack homologous counterparts in vB_EfaS, suggesting the presence of unique genes or genomic elements that may contribute to its distinct biological properties. The combination of moderate nucleotide similarity and partial syntenic conservation indicates that BV26 is related to previously described *Enterococcus* phages but exhibits significant genomic divergence.

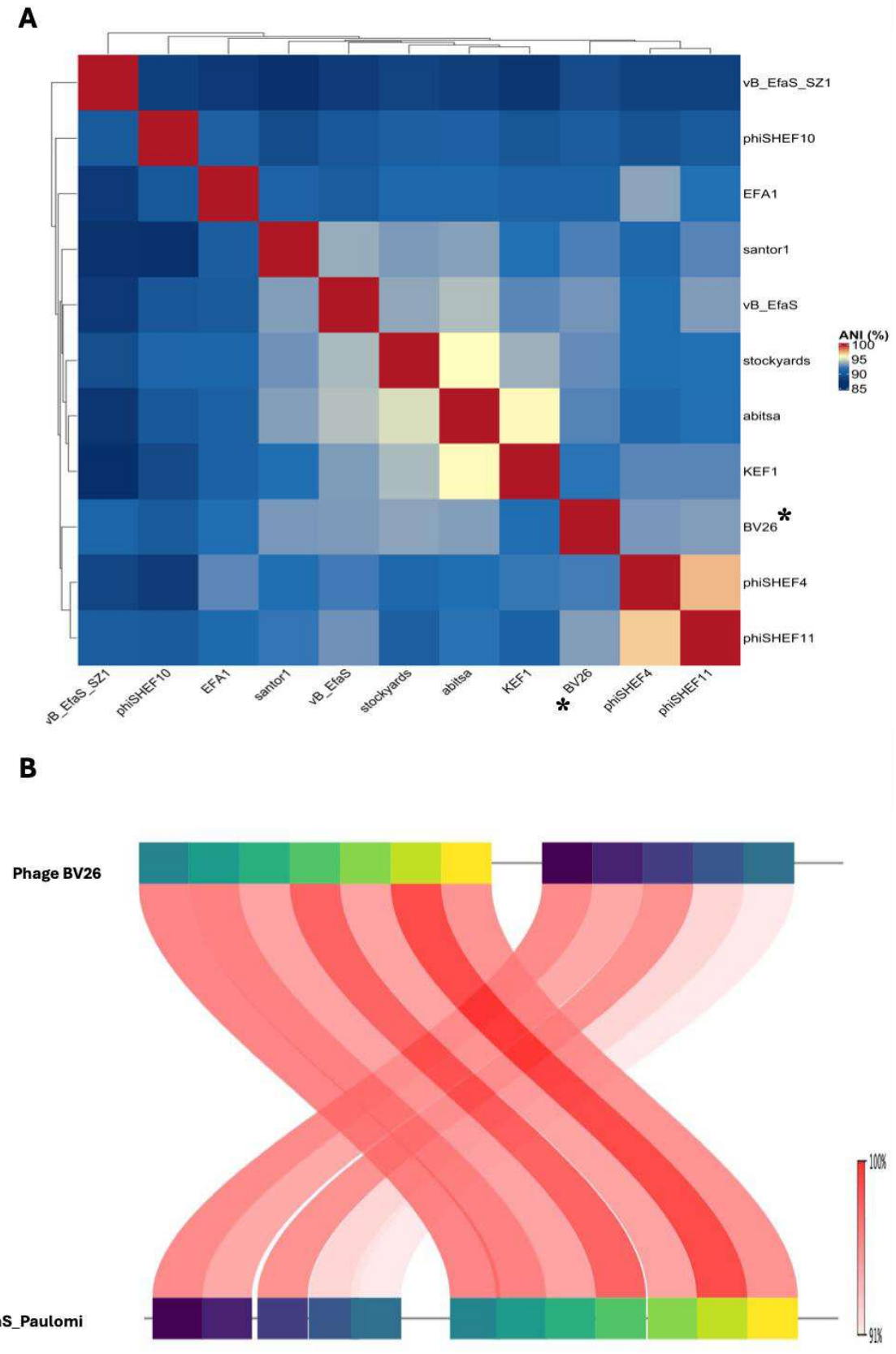

355

356 Fig. 4. Comparative genomic analysis of Enterococcus phage BV26. Heatmap illustrating average
357 nucleotide identity (ANI) values among the isolated phage BV26 (indicated by an asterisk) and

reference *Enterococcus* phages. Color intensity reflects the degree of genomic similarity, ranging from low similarity (dark blue, ~85%) to high similarity (dark red, up to 100%). Distinct clustering patterns highlight genomic relatedness among the analyzed phages (A), and whole-genome alignment of *Enterococcus* phage BV26 and closely related reference phage (vB_EfaS_Paulomi; GenBank accession no. OL539449). Genomes are displayed as linear maps, with predicted protein-coding genes represented by colored arrows. Homologous gene clusters shared among genomes are indicated by similar colors. Ribbons connect homologous regions, with color intensity corresponding to pairwise nucleotide identity (91–100%). Crossed ribbons indicate genomic inversions. Genome sizes are shown using scale bars (10 kb) (B).

3.6. Comparative Proteomic and Phylogenetic Analysis

Proteome-based phylogenetic reconstruction revealed the evolutionary placement of phage BV26 among bacteriophages infecting Gram-positive bacteria (Fig. 5A). The circular phylogenetic tree demonstrates that BV26 clusters within a group of phages associated with *Enterococcus* hosts. However, BV26 occupies a distinct branch within this cluster, indicating a significant degree of proteomic divergence from previously described phages.

Comparative proteome analysis using tBLASTx revealed partial conservation of protein-coding regions between BV26 and other *Enterococcus* phages (Fig. 5B). Several homologous regions were identified across the compared genomes, corresponding primarily to conserved phage functional modules involved in DNA replication, virion morphogenesis, and host cell lysis.

Despite these conserved regions, the overall genomic similarity between BV26 and the compared phages was limited. Multiple genomic segments in the BV26 genome showed little or no detectable similarity with the corresponding regions in the other phages. These regions likely represent unique genes or highly divergent protein sequences that contribute to the distinct genetic composition of BV26.

Among the compared phages, stronger genomic similarity was observed between certain phage pairs, as indicated by extensive homologous links in the tBLASTx comparison. In contrast, BV26 displayed fewer shared homologous regions with the analyzed phages, highlighting its genomic divergence.

Phylogenetic analysis based on the terminase large subunit protein revealed the evolutionary placement of bacteriophage BV26 among related *Enterococcus*-infecting phages (Fig. 6). The generated tree shows that BV26 clusters within the broader group of *Enterococcus* phages but forms a distinct branch separated from closely related reference phages, indicating notable sequence divergence. Although BV26 shares a common ancestor with several *Enterococcus faecalis* phages,

390 the branch length and topology suggest that BV26 has undergone independent evolutionary
391 divergence.

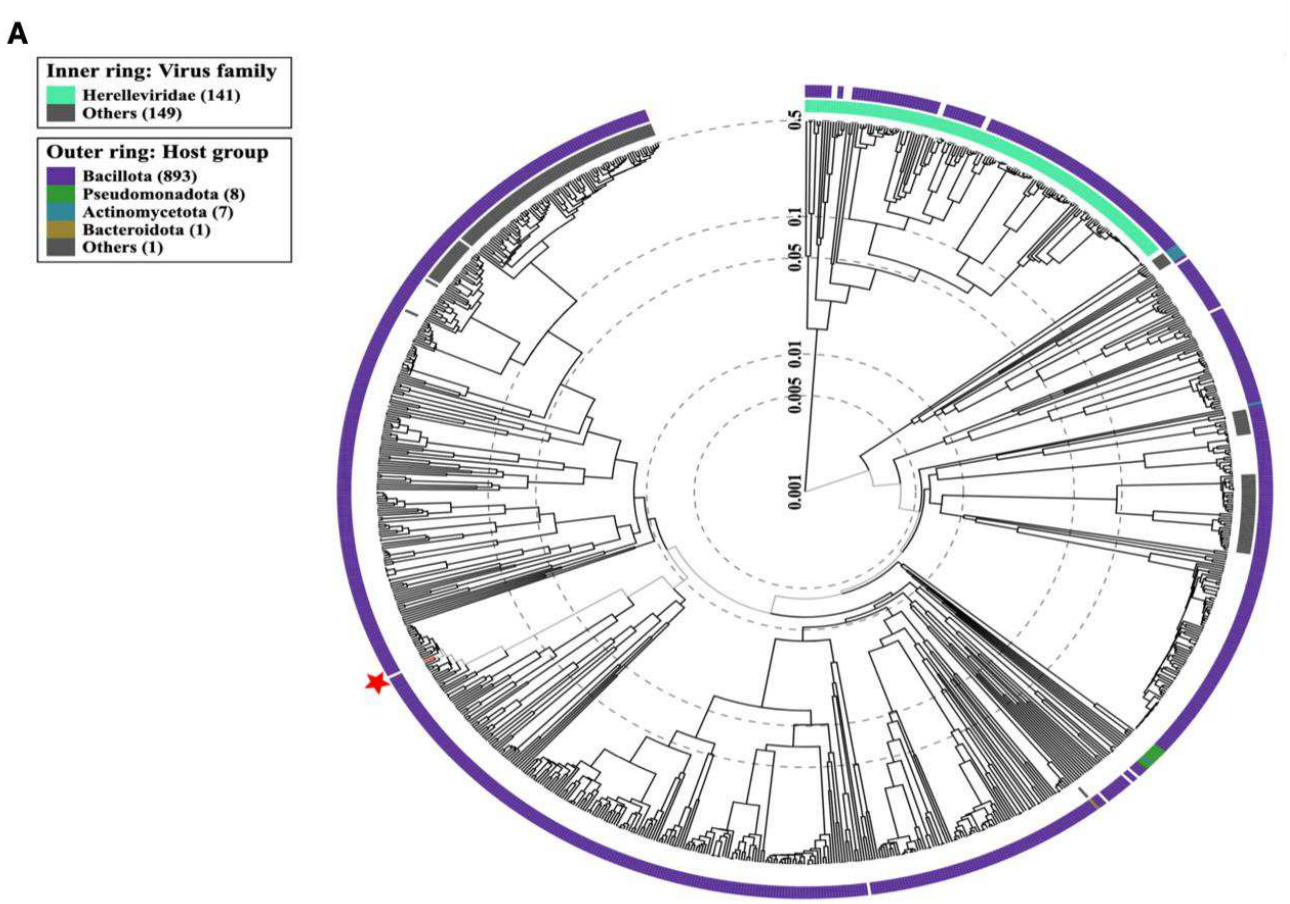
A
Inner ring: Virus family
Herelleviridae (141)
Others (149)
Outer ring: Host group
Bacillota (893)
Pseudomonadota (8)
Actinomycetota (7)
Bacteroidota (1)
Others (1)
0.5
0.1
0.05
0.01
0.005
0.001

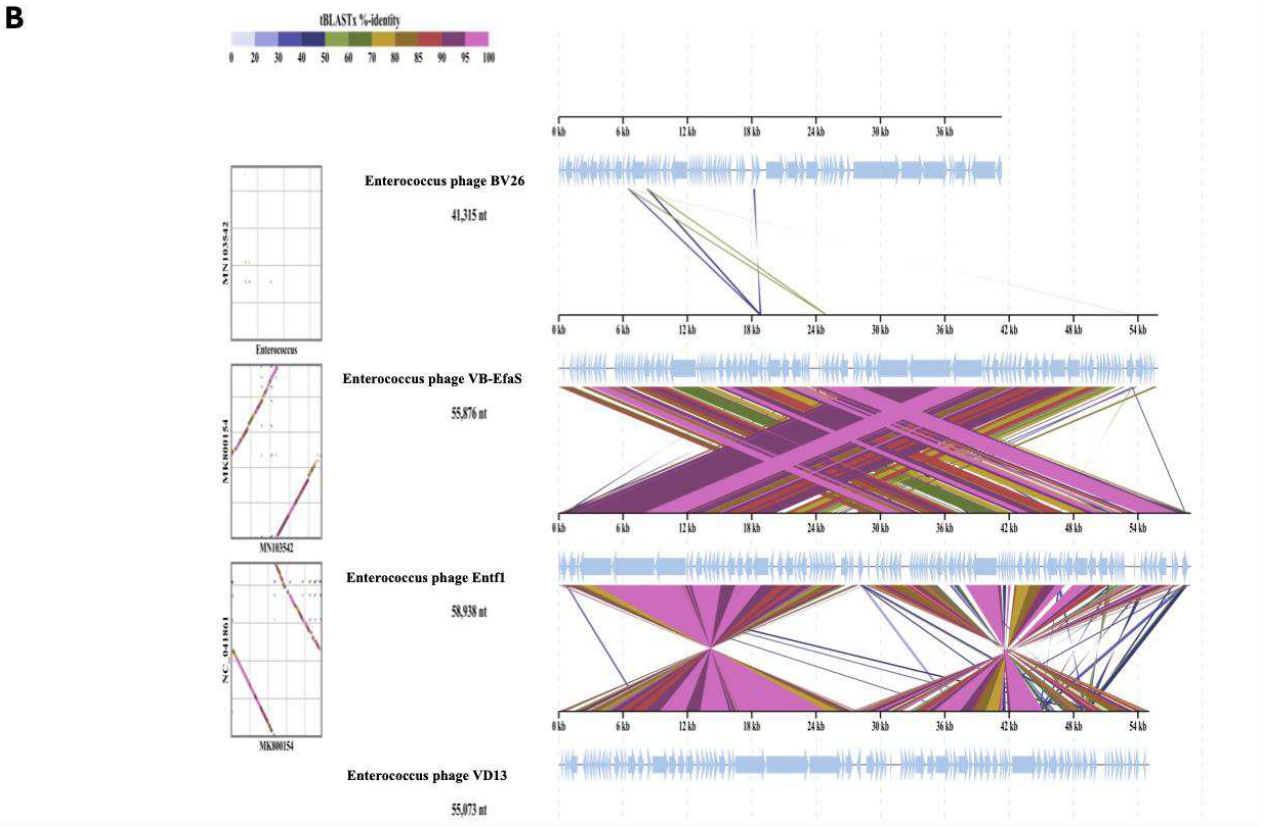
B
tBLASTx %-identity
0 20 30 40 50 60 70 80 85 90 95 100
Enterococcus phage BV26
41,315 nt
Enterococcus phage VB-EfaS
55,876 nt
Enterococcus phage Entf1
58,938 nt
Enterococcus phage VD13
55,073 nt
MN103542
MK800154
NC_041861
Enterococcus
MN103542
MK800154

392

Fig. 5. Comparative proteomic and similarity analysis of phage BV26. Proteome-based phylogenetic tree illustrating the evolutionary relationship of phage BV26 with representative bacteriophages infecting Gram-positive bacterial hosts. The phylogeny was constructed using whole-proteome comparisons, and the circular tree displays the relative placement of BV26 among related phages. The inner ring indicates the virus family classification, while the outer ring represents the host taxonomic groups. The position of BV26 is marked, showing its placement within the cluster of *Enterococcus*-infecting phages (A), and whole-genome comparison between BV26 and selected *Enterococcus* phages using tBLASTx, which compares translated nucleotide sequences across all six reading frames. Colored ribbons represent homologous genomic regions shared among the compared phages, highlighting conserved protein-coding segments (B).

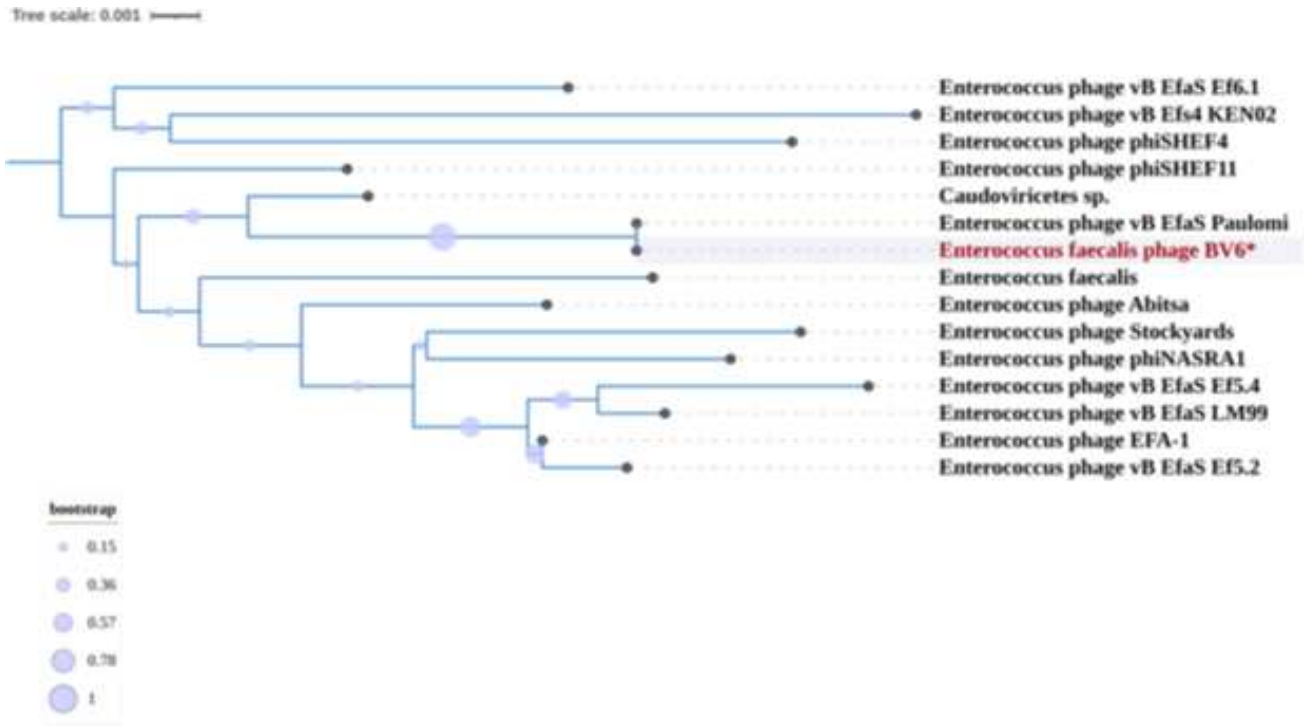

Fig. 6. Phylogenetic analysis of bacteriophage BV26 based on the terminase large subunit protein. A phylogenetic tree was constructed using the amino acid sequences of the terminase large subunit (TerL) from BV26 and related phages infecting Enterococcus species. The tree illustrates the evolutionary relationships among the phages, with branch lengths representing evolutionary distances (scale bar = 0.001 substitutions per site). Bootstrap support values are indicated by circles at the nodes, with circle size proportional to the bootstrap confidence.

3.7. Antibiofilm Activity Assay

The antibiofilm activity of the phage BV26 was evaluated at different multiplicities of infection (MOIs), and a clear dose-dependent reduction in biofilm biomass was observed (Fig. 7).

At the highest MOI (100), the phage treatment resulted in the highest biofilm reduction (P <0.001), with median values exceeding 120% in one condition and approximately 90–100% in the other, indicating highly effective biofilm disruption. As the MOI decreased, the antibiofilm efficacy gradually declined. At MOI=10, biofilm reduction remained substantial, with values ranging around 85–100%, while further decreases were observed at MOI=1, where biofilm reduction dropped to approximately 70–80%. At lower MOIs (0.1 and 0.01), the antibiofilm effect was markedly reduced, with biofilm reduction values falling to approximately 60–70% and 45–55%, respectively. In comparison to 48 h treatment, only the highest MO1 (100) showed a significant reduction in biofilm formation (P <0.001). Despite this decline, phage treatment still demonstrated measurable antibiofilm activity even at the lowest MOI tested. These results demonstrate that the phage exhibits strong antibiofilm activity in an MOI-dependent manner, with maximal efficacy achieved at higher phage concentrations.

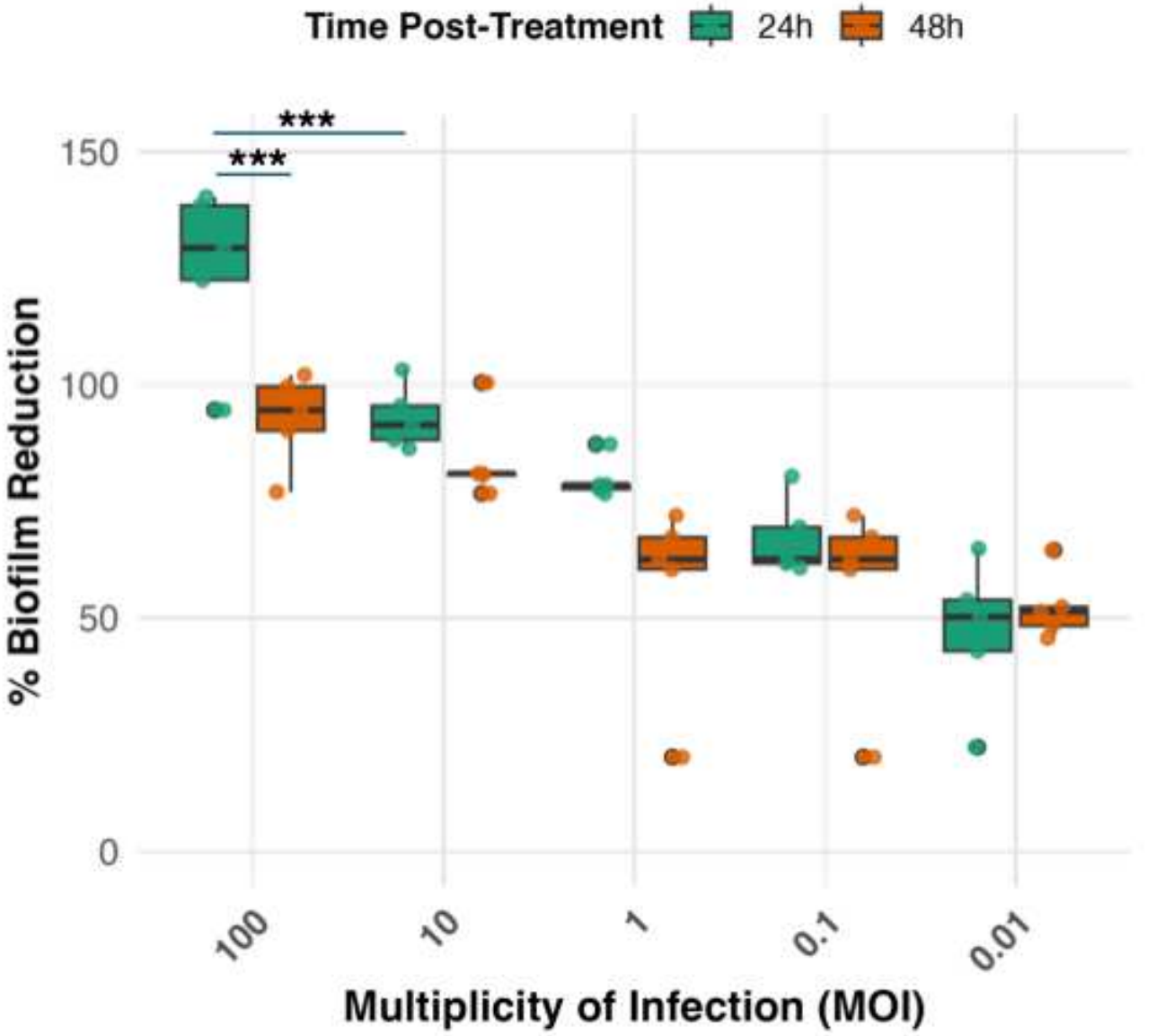

Fig. 7. Dose-dependent effect of phage BV26 on biofilm formation. Biofilm biomass was quantified at different multiplicities of infection (MOI) of phage BV26 at 24 h (green) and 48 h (orange). Boxplots represent the median of six replicates, interquartile range (IQR), and individual data points, illustrating the reduction in biofilm formation with increasing phage concentration. *$P < 0.01$; ***$P < 0.001$; ****$P < 0.0001$.

3.8. Biofilm inhibition potential of phage BV26 against *E. faecalis* on stainless steel food-contact surfaces

The biofilm-inhibiting potential of BV26 phage on stainless steel surface was evaluated at a MOI of 10 in TSB, with the *E. faecalis* CFU/coupon measured at 6 h, 24 h, 3 days, and 5 days. The results revealed that after 6 h of incubation, there was no statistically significant difference (P=0.172) between the control (*E. facealis* only) and the phage-treated samples (*E. faecalis* with phage BV26), with mean

± SD values of 1.57 ± 0.225 and 1.84 ± 0.049 log_{10} CFU/coupon, respectively (Fig. 8a). Indicating that phage BV26 did not substantially affect the initial attachment of *E. faecalis* on stainless steel surface, likely because phage infection had not yet commenced during the early adhesion phase.

At 24 h, both control and phage-treated coupons exhibited a substantial increase in *E. faecalis* count (3-log), with comparable mean ± SD values of 4.08 ± 0.184 and 4.24 ± 0.095 log_{10} CFU/coupon, respectively. The minimal impact of phage treatment during this early stage is likely attributable to the time-dependent nature of the lytic cycle, where phage infection is in its infancy during the initial attachment phase.

Notably, after 72 h of incubation, *E. faecalis* counts in the control group increased markedly, reaching 6.04 ± 0.052 log_{10} CFU/coupon. In contrast, the phage-treated group showed a significant reduction in bacterial density to 3.90 ± 0.071 log_{10} CFU/coupon ($P \leq 0.005$). This inhibitory effect was sustained through day 5, with the phage-treated samples maintaining a significantly lower mean count of 2.40 log_{10} CFU/coupon, whereas the control group remained comparatively high at 5.82 log_{10} CFU/coupon (Fig. 8a).

3.9. Biofilm eradication potential of BV26 phage against *E. faecalis* on stainless steel.

In contrast to the inhibition assay, which evaluated the capacity of phage BV26 to prevent *E. faecalis* biofilm formation, the eradication experiment was designed to assess its efficacy in removing mature biofilms that had been allowed to develop over five days (9.84 log_{10} CFU/coupon) on stainless steel surfaces, with contact times of 1, 3, 6, and 24 h.

The results illustrated in Figure 8b indicate that after the first hour of contact, no significant reduction in *E. faecalis* biofilm was observed between the control and phage-treated groups, with mean values of 9.77 ± 0.12 and 9.21 ± 0.30 log_{10} CFU/coupon, respectively. The number of viable cells within the formed biofilms in the control group remained relatively stable at approximately 9.7 log_{10} CFU/coupon throughout the 24 h exposure period. In contrast, the phage-treated triggered a significant and progressive reduction, showing a ~2-log decrease at 3 h (7.19 ± 0.08 log_{10} CFU/coupon) with a further decline to 5.60 ± 0.21 log_{10} CFU/coupon at 6 h ($P \leq 0.005$).

Significantly, by 24 h, the phage-treated group exhibited an almost complete eradication of the *E. faecalis* biofilm, corresponding to a ~7-log reduction (2.71 ± 0.10 log_{10} CFU/coupon). Demonstrating the BV26 phage's rapid, robust, and sustained anti-biofilm efficacy against mature *E. faecalis* biofilms formed on stainless steel surfaces commonly used in food processing environments.

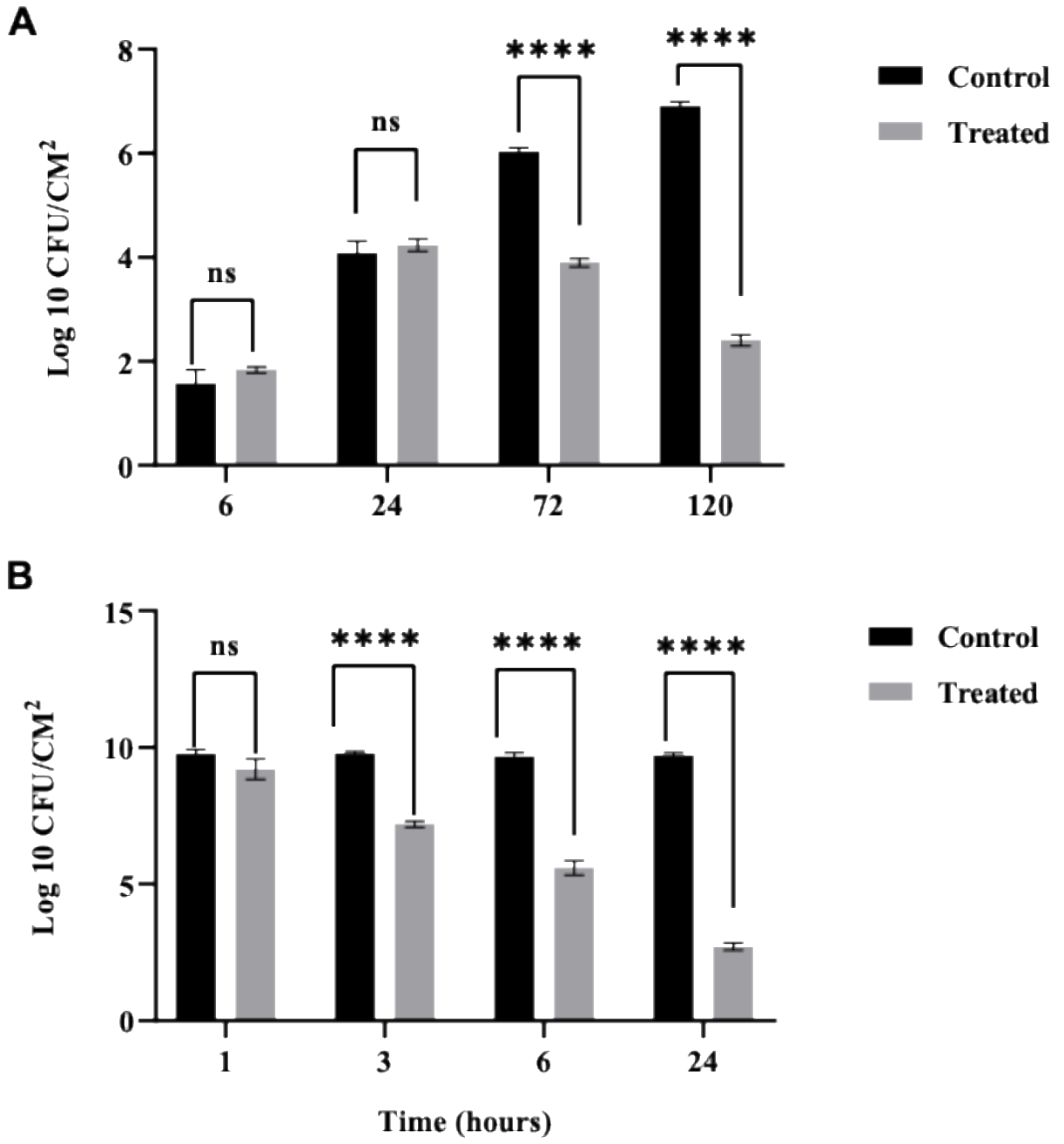

Fig. 8. *E. faecalis* biofilm formation inhibition with BV26 phage on stainless steel sheets (A), and *E. faecalis* biofilm eradication with BV26 phage on stainless steel surfaces after 6 days of biofilm formation (B).

4. Discussion

The present study demonstrates that phage BV26 possesses several characteristics desirable for food-industry biocontrol applications, including broad environmental stability, a genetically safe profile, and strong anti-biofilm activity against *E. faecalis*. Notably, BV26 remained stable under a wide range

of pH, temperature, and UV conditions, lacked detectable virulence and antimicrobial resistance genes, and effectively inhibited and eradicated biofilms on stainless steel surfaces. These findings support the potential of BV26 as a promising alternative strategy for controlling persistent *E. faecalis* contamination in dairy processing environments.

Environmental stability is an important factor when considering bacteriophages for food-processing and other biocontrol applications. In the present study, BV26 and BV34 showed broad pH stability, retaining infectivity from pH 4 to 12, while BV26 remained infective at pH 3, although with reduced activity. Similar stability has been reported for other *E. faecalis*-specific phages isolated from environmental sources. For example, ZXL-01, isolated from lake water, remained stable between pH 4 and 11 and maintained high activity at 60 °C, although its infectivity decreased at 70 °C and was completely lost after 10 min at 80 °C [33]. Likewise, phage ZAT1, isolated from environmental water and identified as an *Efquatrovirus*, showed high survival between pH 4–10 and temperatures of 4–50 °C and remained stable at 4, 37, 50, and 65 °C, with a marked reduction in stability after exposure to 75 °C for 60 min [34]. Similarly, *vB_EfaS_LOK1*, isolated from municipal wastewater, remained stable between 4 and 37 °C, whereas its viability decreased at 60 and 70 °C and was completely lost at 80 °C [35] . Consistent with these observations, both BV26 and BV34 remained stable up to 50 °C and showed a gradual decline in infectivity at higher temperatures rather than an abrupt loss of activity. Complete inactivation was observed only at 80 °C for BV34. This thermal tolerance appears comparatively favorable to that reported in some previous studies, as Victoria-Blanco et al. (2024) similarly observed complete loss of infectivity at 80 °C [36], whereas González-Gómez et al. (2024) reported rapid loss of activity above 60 °C, with their nine phages unable to tolerate 70 °C **[37]**. Similarly, Abed et al. (2024) reported complete inactivation of an *E. faecalis* phage at temperatures above 50 °C[38]. Overall, the broad pH tolerance and relatively high thermal stability of BV26 and BV34 suggest that these phages can withstand a wider range of environmental conditions than some previously reported *E. faecalis* phages, supporting their potential application in dairy-processing environments where fluctuations in pH and moderate heat exposure may occur.

Resistance to UV irradiation is another desirable property for phages intended for industrial applications. Remarkably, both BV26 and BV34 retained full infectivity after 60 min of exposure to UV radiation, whereas the phage described by Victoria-Blanco et al. (2024) lost viability within one minute [36] . This exceptional UV tolerance suggests that these phages could remain effective even in environments routinely subjected to UV surface sterilization or food decontamination procedures. Supporting this concept, Myshkevych et al. (2025) demonstrated that combining UV treatment with bacteriophages significantly enhanced bacterial removal in anaerobic bioreactors compared with

conventional cleaning alone [39]. The remarkable UV stability of BV26 and BV34 indicates that they could be integrated with existing sanitation strategies without compromising their biological activity.

Whole-genome sequencing confirmed that BV26 possesses a 41,165 bp double-stranded DNA genome with a GC content of 34.91%, consistent with other *Enterococcus* phages belonging to the class *Caudoviricetes* [40]. Genome completeness assessment using both AAI- and HMM-based approaches confirmed that the assembled genome was complete and free from bacterial DNA contamination. Importantly, no virulence factors, antimicrobial resistance genes, or lysogeny-associated genes were identified, supporting the strictly lytic nature of BV26 and reinforcing its suitability for biocontrol applications, where genome safety is a critical requirement [41].

Genome annotation revealed the characteristic modular organization commonly observed in tailed bacteriophages. Structural genes represented the largest functional category and included capsid, tail, and capsid maturation proteins essential for virion assembly. DNA packaging genes encoding the terminase subunits and replication-associated proteins further demonstrated that BV26 possesses a complete infection machinery comparable to that reported for members of the *Herelleviridae* family[42]. The identification of both holin and lysin homologs suggests that BV26 employs the classical two-component lysis mechanism, in which holins permeabilize the bacterial membrane, allowing lysins to degrade the peptidoglycan layer and release progeny phages[43].

Despite the comprehensive genome annotation, more than half of the predicted coding sequences encoded hypothetical proteins with no assigned biological function. Similar observations have been reported for numerous bacteriophage genomes and reflect the extensive "viral dark matter" that remains functionally unexplored [44]. Future transcriptomic and proteomic investigations will be valuable for elucidating the roles of these uncharacterized proteins during the phage infection cycle.

Comparative genomic analysis demonstrated that BV26 shared its highest average nucleotide identity (91%) with phage vB_EfaS_Paulomi. Although this indicates a close evolutionary relationship, the value remains below the commonly accepted 95% threshold for species delineation [45, 46]. Together with the extensive genomic rearrangements observed in the synteny analysis, these findings strongly suggest that BV26 represents a distinct *Enterococcus* bacteriophage. Proteome-based phylogenetic reconstruction using ViPTree and phylogenetic analysis of the conserved terminase large subunit consistently placed BV26 within the *Enterococcus* phage cluster while forming an independent evolutionary branch. Collectively, these genomic and phylogenetic analyses support the classification of BV26 as a novel bacteriophage.

The antibiofilm assays further demonstrated the strong biocontrol potential of BV26. Biofilm inhibition occurred in a clear MOI-dependent manner, with reductions exceeding 95% at an MOI of 100 after both 24 and 48 h of incubation. Comparable antibiofilm activity has been reported for phage EFDG1, which reduced *E. faecalis* biofilms by approximately 80–90% at high MOIs [47]. Notably, BV26 retained measurable antibiofilm activity even at MOIs as low as 0.01 and 0.1, indicating efficient phage replication within the developing biofilm. This observation is consistent with the phenomenon of phage amplification, whereby newly produced phage particles propagate throughout the biofilm and progressively infect neighboring bacterial cells, allowing substantial biofilm disruption even from low initial phage doses [48].

Since stainless steel is the predominant material used in dairy processing equipment, evaluating phage performance on this surface is essential for assessing industrial applicability. Mature *E. faecalis* biofilms formed on stainless steel are notoriously difficult to eliminate due to their increased tolerance to disinfectants and their ability to act as persistent reservoirs of contamination [49]. In the present study, BV26 had little effect on the initial adhesion of *E. faecalis* during the first 24 h, likely because phage infection requires metabolically active cells to complete adsorption, genome injection, and intracellular replication [50]. However, once biofilm development progressed, BV26 significantly suppressed bacterial colonization, reducing biofilm density by approximately 4 $\log_{10}$ CFU/coupon after five days. Similar findings were reported by [17], who demonstrated substantial degradation of extracellular polymeric substances in *E. faecalis* biofilms following phage treatment, while [51] observed comparable antibiofilm activity in both broth and milk models. These results suggest that higher phage concentrations or phage pre-treatment strategies may further improve prevention of early bacterial attachment.

The ability to eradicate established biofilms is particularly important in food-processing facilities, where mature biofilms are responsible for persistent contamination and recurrent equipment colonization [52, 53]. BV26 exhibited remarkable efficacy against mature five-day-old *E. faecalis* biofilms, achieving an approximately 7 $\log_{10}$ CFU/coupon reduction within only 24 h. This performance compares favorably with previous reports. [54] observed a 6 $\log_{10}$ CFU/cm² reduction in mature *Escherichia coli* biofilms following phage treatment, whereas [55, 56] reported effective biofilm disruption after prolonged incubation under broth conditions. Direct evaluation of phage-mediated eradication of *E. faecalis* biofilms on stainless steel remains scarce, highlighting the practical significance of the present findings. The potent inhibition and eradication activities demonstrated by

BV26 underscore its promise as a natural, targeted, and environmentally friendly strategy for improving hygiene and biofilm management in dairy processing environments.

Overall, these findings demonstrate that phage BV26 is a safe, genetically distinct, and highly effective anti-biofilm agent with considerable potential for controlling *E. faecalis* contamination on food-contact surfaces, supporting its future development as a sustainable biocontrol strategy for improving hygiene and food safety in dairy processing environments.

5. Conclusion

This study identified and comprehensively characterized a novel lytic *Enterococcus* phage, BV26, with promising potential for controlling *E. faecalis* in dairy processing environments. BV26 exhibited remarkable environmental stability across a broad range of pH values, temperatures, and UV exposure, while whole-genome sequencing confirmed the absence of virulence factors, antimicrobial resistance genes, and lysogeny-associated genes, supporting its safety for biocontrol applications. Comparative genomic and phylogenetic analyses further demonstrated that BV26 represents a genetically distinct *Enterococcus* phage. Functionally, BV26 displayed potent antibiofilm activity by significantly inhibiting biofilm formation in an MOI-dependent manner and effectively eradicating mature *E. faecalis* biofilms formed on stainless steel surfaces, achieving up to a 7-$\log_{10}$ reduction in bacterial counts within 24 h. Collectively, these findings highlight BV26 as a safe, stable, and highly effective biocontrol agent with considerable potential for improving hygiene and mitigating persistent *E. faecalis* contamination in dairy processing facilities. Future studies should evaluate its efficacy under industrial processing conditions and explore its integration with existing sanitation strategies to facilitate practical implementation in the food industry.

Declarations

Authorship contribution statement

D.E.: Conceptualization, Methodology, Investigation, Formal analysis, Data curation, Writing – review & editing. **R.S.M.**: Methodology, Investigation, Formal analysis, Data curation. **M.N.A.:**

Methodology, Investigation, Formal analysis, Data curation, Writing – review & editing. **M.G.:** Methodology, Investigation, Formal analysis, Data curation. **M.E.:** Data curation, Writing – review & editing**, Y.M.:** Methodology, Investigation, Writing – review & editing**, K.H.:** Methodology, Investigation, Writing – review & editing**, E.M.T.:** Conceptualization, Methodology, Investigation, Formal analysis, Data curation, Writing – review & editing

Dina El-Sayed[a], Rasha Samir Mohamed[a], Marwa N. Ahmed[b,a*], Mokhtar Gomaa[c], Mohamed El-Telbany [d], Yoshimitsu Masuda[e], Ken-ichi Honjoh[e], Eman M. Taher

Declaration of competing interest

The authors declare that they have no known competing financial interests or personal relationships that could have appeared to influence the work reported in this paper.

Funding Sources

This research did not receive any specific grant from funding agencies in the public, commercial, or not-for-profit sectors.

Data availability

Data will be made available on request.

References

1. Taher, E.M., et al., *Molecular characterization of antimicrobial resistance genes on farms and in commercial milk with emphasis on the effect of currently practiced heat treatments on viable but nonculturable formation*. Journal of Dairy Science, 2020. **103**(11): p. 9936-9945.
2. El-Zayat, A.S., et al., *Seasonal prevalence of extended-spectrum β-lactamase–producing bacteria in food-chain animals, humans, and the surrounding environment in Fayoum governorate: a one health approach*. Frontiers in Microbiology, 2026. **17**: p. 1726798.
3. Ahmed, M.N., et al., *Formulation and evaluation of therapeutic antimicrobial citrus and Manuka honey creams with aloe vera, mint essential oil, and Indian costus*. Scientific Reports, 2025. **15**(1): p. 7477.
4. Awad, E.H., et al., *Unveiling the anti-biofilm potential of bee venom against multi-drug resistant human pathogenic bacteria and fungi: perspectives into the efficacy and possible mechanisms*. Microbial pathogenesis, 2025. **200**: p. 107358.
5. Ibrahim, N., et al., *Chemical profiling, molecular docking, and harnessing Manuka honey's antimicrobial and prebiotic potential in probiotic milk and yoghurt*. Food Microbiology, 2026: p. 105045.
6. Koskeroglu, K., et al., *Tracking persistent and resistant Enterococcus faecalis and E. faecium from farm to fork: biofilm-linked risks in antibiotic resistance of isolates*. Vet Res Commun, 2026. **50**(2): p. 100.
7. da Silva Fernandes, M., D.Y. Kabuki, and A.Y. Kuaye, *Biofilms of Enterococcus faecalis and Enterococcus faecium isolated from the processing of ricotta and the control of these pathogens through cleaning and sanitization procedures*. International Journal of Food Microbiology, 2015. **200**: p. 97-103.
8. Yang, S., et al., *Strategies and mechanisms targeting Enterococcus faecalis biofilms associated with endodontic infections: a comprehensive review*. Front Cell Infect Microbiol, 2024. **14**: p. 1433313.

9. LaPointe, G., et al., *Biofilm Formation in Dairy: A Food Safety Concern—Microbial community tracking from dairy farm to factory; Insights on biofilm management for enhanced food safety and quality.* Journal of Dairy Science, 2025. **108**(8): p. 8101-8119.
10. Diarra, C., et al., *Biofilm formation by heat-resistant dairy bacteria: multispecies biofilm model under static and dynamic conditions.* Applied and Environmental Microbiology, 2023. **89**(10): p. e00713-23.
11. de Castro, M.R., et al., *Biofilm formation on stainless steel as a function of time and temperature and control through sanitizers.* International dairy journal, 2017. **68**: p. 9-16.
12. Vadakkan, K., et al., *A critical review on innovative targets for signal disruption in Enterococcus faecalis infection management.* Microbial Pathogenesis, 2025. **207**: p. 107876.
13. Linares, D.M., et al., *Comparative analysis of the in vitro cytotoxicity of the dietary biogenic amines tyramine and histamine.* Food Chemistry, 2016. **197**: p. 658-663.
14. Yan, X., et al., *Sublethal sanitizers exposure differentially affects biofilm formation in three adapted Salmonella strains: A phenotypic-transcriptomic analysis of increased biofilm formed by ATCC 14028.* Int J Food Microbiol, 2025. **436**: p. 111189.
15. El-Sayed, D.G., et al., *Isolation and characterization of novel phages for control of the phytopathogen Pseudomonas marginalis.* Applied Microbiology and Biotechnology, 2025. **109**(1): p. 276.
16. El-Telbany, M., et al., *Enterococci in food: Risks and phage-based control strategies.* The Microbe, 2025. **8**: p. 100544.
17. Moryl, M., et al. *How Do Phages Disrupt the Structure of Enterococcus faecalis Biofilm?* International Journal of Molecular Sciences, 2023. **24**, 17260 DOI: 10.3390/ijms242417260.
18. Kropinski, A.M., et al., *Enumeration of Bacteriophages by Double Agar Overlay Plaque Assay*, in *Bacteriophages: Methods and Protocols, Volume 1: Isolation, Characterization, and Interactions*, M.R.J. Clokie and A.M. Kropinski, Editors. 2009, Humana Press: Totowa, NJ. p. 69-76.
19. Adams, M.H., *Bacteriophages.* 1959.
20. El-Sayed, D., et al., *Evaluating the phenotypic and genomic characterization of some Egyptian phages infecting Shiga Toxin-Producing Escherichia coli O157: H7 for the prospective application in food Bio-Preservation.* Biology, 2022. **11**(8): p. 1180.
21. Chen, S., et al., *fastp: an ultra-fast all-in-one FASTQ preprocessor.* Bioinformatics, 2018. **34**(17): p. i884-i890.
22. Nayfach, S., et al., *CheckV assesses the quality and completeness of metagenome-assembled viral genomes.* Nature Biotechnology, 2021. **39**(5): p. 578-585.
23. Arndt, D., et al., *PHASTER: a better, faster version of the PHAST phage search tool.* Nucleic Acids Research, 2016. **44**(W1): p. W16-W21.
24. Wishart, D.S., et al., *PHASTEST: faster than PHASTER, better than PHAST.* Nucleic Acids Research, 2023. **51**(W1): p. W443-W450.
25. Alcock, B.P., et al., *CARD 2023: expanded curation, support for machine learning, and resistome prediction at the Comprehensive Antibiotic Resistance Database.* Nucleic Acids Research, 2023. **51**(D1): p. D690-D699.
26. Chen, L., et al., *VFDB: a reference database for bacterial virulence factors.* Nucleic Acids Research, 2005. **33**(suppl_1): p. D325-D328.

27. Wang, R.H., et al., *PhageScope: a well-annotated bacteriophage database with automatic analyses and visualizations*. Nucleic Acids Research, 2024. **52**(D1): p. D756-D761.
28. Grant, J.R., et al., *Proksee: in-depth characterization and visualization of bacterial genomes*. Nucleic Acids Research, 2023. **51**(W1): p. W484-W492.
29. Nishimura, Y., et al., *ViPTree: the viral proteomic tree server*. Bioinformatics, 2017. **33**(15): p. 2379-2380.
30. Thompson, J.D., D.G. Higgins, and T.J. Gibson, *CLUSTAL W: improving the sensitivity of progressive multiple sequence alignment through sequence weighting, position-specific gap penalties and weight matrix choice*. Nucleic Acids Research, 1994. **22**(22): p. 4673-4680.
31. Letunic, I. and P. Bork, *Interactive Tree of Life (iTOL) v6: recent updates to the phylogenetic tree display and annotation tool*. Nucleic Acids Research, 2024. **52**(W1): p. W78-W82.
32. Santiago, A.J., et al., *Inhibition and Dispersal of Pseudomonas aeruginosa Biofilms by Combination Treatment with Escapin Intermediate Products and Hydrogen Peroxide*. Antimicrob Agents Chemother, 2016. **60**(9): p. 5554-62.
33. Jiang, H., et al., *Isolation and Characterization of Enterococcus faecalis Phage ZXL-01 and Preliminary Investigation of Its Therapeutic Effect on Periapical Periodontitis*. Current Issues in Molecular Biology, 2025. **47**(6): p. 469.
34. Ali, Z., et al., *Therapeutic potential of a newly isolated bacteriophage against multi-drug resistant Enterococcus faecalis infections: in vitro and in vivo characterization*. BMC Microbiol, 2025. **25**(1): p. 80.
35. Plata Suarez, L.M., et al., *Unlocking the Potential of vB_EfaS_LOK1: A Newly Isolated Bacteriophage Against Enterococcus faecalis*. Microorganisms, 2025. **13**(10): p. 2414.
36. Victoria-Blanco, E.E., et al., *Characterization of Enterobacter phage vB_EcRAM-01, a new Pseudotevenvirus against Enterobacter cloacae, isolated in an urban river in Panama*. Plos one, 2024. **19**(12): p. e0310824.
37. González-Gómez, J.P., et al., *Genomic and biological characterization of bacteriophages against Enterobacter cloacae, a high-priority pathogen*. Virology, 2024. **595**: p. 110100.
38. Abed, S., et al., *Insights into the novel Enterococcus faecalis phage: A comprehensive genome analysis*. Plos one, 2024. **19**(5): p. e0301292.
39. Myshkevych, Y., et al., *Effectiveness of combined UV-C and bacteriophage approach over repeated cleaning cycles to alleviate membrane fouling of anaerobic bioreactors*. Chemical Engineering Journal Advances, 2025: p. 100796.
40. Chen, Q., et al., *Isolation and characterization of a novel Enterococcus phage Phi_Eg_SY1*. Virus Research, 2023. **332**: p. 199132.
41. Hatfull, G.F., *Bacteriophage genomics*. Current opinion in microbiology, 2008. **11**(5): p. 447-453.
42. Mäntynen, S., et al., *Black box of phage–bacterium interactions: exploring alternative phage infection strategies*. Open Biology, 2021. **11**(9).
43. Young, R., *Phage lysis: three steps, three choices, one outcome*. Journal of microbiology, 2014. **52**(3): p. 243-258.
44. Roux, S., et al., *Viral dark matter and virus–host interactions resolved from publicly available microbial genomes*. elife, 2015. **4**: p. e08490.
45. Kim, M., et al., *Towards a taxonomic coherence between average nucleotide identity and 16S rRNA gene sequence similarity for species demarcation of prokaryotes*. International journal of systematic and evolutionary microbiology, 2014. **64**(Pt_2): p. 346-351.

46. Simmonds, P., et al., *Virus taxonomy in the age of metagenomics: consensus statement*. Nature Reviews Microbiology, 2017. **15**(3): p. 161-168.
47. Khalifa, L., et al., *Targeting Enterococcus faecalis biofilms with phage therapy.* Applied and environmental microbiology, 2015. **81**(8): p. 2696-2705.
48. Pires, D.P., L.D. Melo, and J. Azeredo, *Understanding the complex phage-host interactions in biofilm communities*. Annual Review of Virology, 2021. **8**(1): p. 73-94.
49. Sadanandan, B. and K.M. Yogendraiah, *Enterococcus faecalis Biofilm: A Clinical and Environmental Hazard*. Medical Sciences Forum, 2025. **35**(1): p. 5.
50. Liu, S., et al., *Phages against Pathogenic Bacterial Biofilms and Biofilm-Based Infections: A Review.* Pharmaceutics, 2022. **14**(2).
51. El-Telbany, M., et al., *Potential application of phage vB_EfKS5 to control Enterococcus faecalis and its biofilm in food*. AMB Express, 2023. **13**(1): p. 130.
52. Cherif Anntar, A., et al., *Assessment of the efficiency of cleaning and disinfection protocols against Enterococcus faecalis biofilms recovered from milk pipes*. Journal of Food Safety and Food Quality-Archiv für Lebensmittelhygiene, 2024. **73**: p. 172-179.
53. Taher, E.M., T. Veltman, and K.R. Petrovski, *Presence of Bacillus species in pasteurised milk and their phenotypic and genotypic antimicrobial resistance profile.* International Journal of Dairy Technology, 2023. **76**(1): p. 63-73.
54. González-Gómez, J.P., et al., *Efficacy of novel bacteriophages against Escherichia coli biofilms on stainless steel*. Antibiotics, 2021. **10**(10): p. 1150.
55. Soro, O., et al., *Characterization and Anti-Biofilm Activity of Lytic Enterococcus Phage vB_Efs8_KEN04 against Clinical Isolates of Multidrug-Resistant Enterococcus faecalis in Kenya*. Viruses, 2024. **16**(8).
56. El-Atrees, D.M., et al., *Characterization and anti-biofilm activity of bacteriophages against urinary tract Enterococcus faecalis isolates*. Scientific Reports, 2022. **12**(1): p. 13048.

Supplementary Files

This is a list of supplementary files associated with this preprint. Click to download.

- TableS1Supplementaryfile.docx